

Fusion Between Frozen-Wave-Type Beams and Airy-Type Pulses: Diffraction-Dispersion-Attenuation Resistant Vortex Pulses in Absorbing Media

Michel Zamboni-Rached^{1*} and Mo Mojahedi²

November 27, 2024

¹University of Campinas, Campinas, SP, Brazil.

²Department of Electrical and Computer Engineering at the University of Toronto, Toronto, ON, Canada.

Abstract

In this paper we perform a fusion between two important theoretical methodologies, one related to the Frozen Wave beams, which are non-diffracting beams whose longitudinal intensity pattern can be chosen *a priori* in an medium (absorbing or not), and the other related to the Airy-Type pulses, which are pulses resistant to dispersion effects in dispersive materials. As a result, a new method emerges, capable of providing vortex pulses resistant to three concomitant effects, i.e.: diffraction, dispersion and attenuation; while concurrently the spatial variation of the wave intensity along its axis of propagation can be engineered at will. The new approach can be seen as a generalization of the Localized Waves theory in the paraxial regime and the new pulses can have potential applications in different fields such as optics communications, nonlinear optics, micromanipulation, and so on.

1 Introduction

Since the works of Sheppard and Wilson [1], Brittingham [2] and Durnin [3], the subject of non-diffracting beams and pulses, also known as Localized Waves, has been of interest to many researches. It is now a well established fact that non-diffracting waves [4, 5] such as the Bessel beams can resist diffraction effects for long distances, when compared to the ordinary waves. Moreover, in Ref. [6] it was shown that it is possible to model the longitudinal intensity pattern of the non-diffracting beams at will, in an approach dubbed *Frozen Waves* (FWs). Such intensity pattern, chosen *a priori*, can be constructed on axis ($\rho = 0$) or on the surface of a cylinder [7] of radius $\rho = \rho_\nu$, where the resulting beams – called Frozen Waves (FWs) – were experimentally demonstrated in Refs. [8, 9]. Later, the FW method was extended in [10, 11], allowing the spatial shaping of non-diffracting beams to take place in absorbing materials. That was an important step forward in the Localized Wave theory, as it provided beams not only resistant to the diffraction but also to the attenuation. The theoretical finite energy version of diffraction-attenuation resistant beams was developed in [12, 13], and later on it was shown (theoretically and experimentally) that FW beams can be used to control the orbital angular momentum (OAM) [14] and the polarization [15, 16] of a beam along its axis of propagation. In short, today, FWs can be understood as a class of structured light in which the beam's intensity pattern, polarization, OAM (magnitude and sign), and wavelength can be engineered, almost at will, along its axis of propagation.

*E-mail address for contacts: mzamboni@decom.fee.unicamp.br

As related to pulses and their resistance to diffraction, they have been discussed in Refs. [2,17-30], where the theory was later extended to include pulses resistant to both diffraction and dispersion [31-38]. However, in order to adorn the above mentioned pulses with a degree of resistance toward dispersion, a complicated space-time coupling in their spectra was needed. But, with the advent of Airy pulses the situation became relatively simpler since such pulses only required a suitable cubic phase in the frequency spectrum [39-44]

In summary, today, within the Localized Wave theory, we have: i) beams that can resist diffraction and attenuation effects when propagating in unguided absorbing media, and ii) pulses resistant to the diffraction and dispersion effects in unguided dispersive media. In light of our previous discussion regarding FWs and structured light, naturally, a question can be asked: is it possible to engineer a vortex pulse that is concurrently resistant to the three concomitant effects of diffraction, dispersion and attenuation in unguided dispersive absorbing media, while at same time – similar to the case of FWs – the pulse intensity can display priorly chosen values at different locations (regions) along its direction of propagation? Undoubtedly, demonstrating such capability can open new venues for other possibilities such as engineering the pulse polarization, (local) OAM and central wavelength along the propagation. However, these particular considerations will be postponed to future communications.

In this paper, we show that it is possible to construct pulses that, over a finite distance, are immune to diffraction, dispersion and attenuation while, at same time, their intensities can assume arbitrary values and patterns along the propagation. The paper is organized as the following. In section 2, we develop the required theoretical frame work, whereas section 3 describes some of the applicable examples. Section 4 contains our final remarks and conclusions. We expect that the theoretical formulation presented here will have an important impact in multiple areas of research in optical sciences such as optical communications, non-linear optics and optical manipulations.

2 The Method

Let us first present the basic equations that describe the evolution of a pulse in a linear media. A pulse, $\Psi(\mathbf{r}, t)$, with slowly varying envelope, propagating in a dispersive absorbing medium with complex index of refraction, $n(\omega) = n_R(\omega) + in_I(\omega)$, can be described as:

$$\Psi(\mathbf{r}, t) = e^{ik(\omega_0)z} e^{-i\omega_0 t} A(\mathbf{r}, t), \quad (1)$$

with

$$k(\omega_0) = n_R(\omega_0) \frac{\omega_0}{c} + in_I(\omega_0) \frac{\omega_0}{c} = k_R(\omega_0) + ik_I(\omega_0) \equiv k_{R0} + ik_{I0}. \quad (2)$$

The pulse envelope, $A(\mathbf{r}, t)$, obeys

$$\frac{1}{2k(\omega_0)} \nabla_{\perp}^2 A + i \left(\frac{\partial}{\partial z} + \beta_1 \frac{\partial}{\partial t} \right) A - \frac{\beta_2}{2} \frac{\partial^2 A}{\partial t^2} = 0, \quad (3)$$

where

$$\beta_1 = \frac{\partial k_R}{\partial \omega} \Big|_{\omega_0} \quad \text{and} \quad \beta_2 = \frac{\partial^2 k_R}{\partial \omega^2} \Big|_{\omega_0}. \quad (4)$$

By making the usual transformations, $z = z$ and $T = t - z/v_g$, with $v_g = 1/\beta_1$, we can rewrite Eq.(3) as

$$\frac{1}{2k(\omega_0)} \nabla_{\perp}^2 A + i \frac{\partial}{\partial z} A - \frac{\beta_2}{2} \frac{\partial^2 A}{\partial T^2} = 0. \quad (5)$$

Now, let us consider the pulse envelope, $A(\mathbf{r}, t)$, having the following form

$$A(\mathbf{r}, t) = W(\rho, \phi, z) P(z, T). \quad (6)$$

By substituting Eq.(6) in (5), we have

$$\frac{1}{2k(\omega_0)} \nabla_{\perp}^2 W + i \frac{\partial W}{\partial z} = 0, \quad (7)$$

and

$$i \frac{\partial P}{\partial z} - \frac{\beta_2}{2} \frac{\partial^2 P}{\partial T^2} = 0. \quad (8)$$

At this point it is important to note that $W(\rho, \phi, z)$, governed by Eq.(7), is the partial differential equation for the envelope of a paraxial beam; while $P(z, T)$, governed by Eq.(8), is the partial differential equation for the envelope of a 1D pulse propagating in a dispersive medium.

Having established the differential equations governing the behavior of $W(\rho, \phi, z)$ and $P(z, T)$, in the next subsection we will develop a space-time modeling of vortex pulses (i.e. pulses carrying OAM) propagating in unguided, dispersive, and absorbing medium. Consequently, we shall see that it is possible to construct vortex pulses which resist the effects of dispersion, diffraction, and attenuation as they propagate in an unbounded medium. Such construction and formulation can be viewed as the generalization of the Localized Wave theory in the paraxial regime.

2.1 Space-time Modeling of Diffraction, Dispersion, and Attenuation Resistant Vortex Pulses

The basic approach in developing vortex pulses, $A(\mathbf{r}, t)$, that are immune to diffraction, attenuation, and dispersion is to enforce resistance to diffraction and attenuation (along with control of the OAM) through the spatial function $W(\rho, \phi, z)$ and its corresponding differential equation, Eq.(7); whereas to make the vortex pulses resistant to dispersion through the temporal function, $P(z, T)$, and its corresponding differential equation, Eq.(8).

Similar to the approach in [12], we choose $W(\rho, \phi, z)$ to be a superposition of $2N + 1$ copropagating ν -order Bessel-Gauss beams given by

$$W(\rho, \phi, z) = \frac{\exp\left(-q^2 \frac{\rho^2}{\mu}\right)}{\mu} \exp\left(-ik(\omega_0) \frac{z}{\mu}\right) \sum_{m=-N}^N A_m J_{\nu}\left(\eta_m \frac{\rho}{\mu}\right) e^{i\nu\phi} \exp\left(i\zeta_m \frac{z}{\mu}\right), \quad (9)$$

where

$$\mu = 1 + i2 \frac{q^2}{k(\omega_0)} z. \quad (10)$$

In Eq.(9), q is a constant, A_m are coefficients of expansions to be determined, and η_m and ζ_m are the transverse and longitudinal wavenumbers (respectively) of the m th Bessel-Gauss beam in the superposition that must satisfy $\zeta_m = k(\omega_0) - \eta_m^2/2k(\omega_0)$.

The solution (9) can be used for obtaining a light beam, given by $\exp(-k_{I0}z)\exp(ik_{R0}z - i\omega_0 t)W(\rho, \phi, z)$, resistant to the diffraction and attenuation effects in an absorbing medium, with a longitudinal intensity pattern that can be chosen *a priori*. This intensity pattern is given by a function, $|F(z)|^2$, of our choice, and can be concentrated over the z axis (in the case $\nu = 0$), with a beam spot radius r_0 , or over a cylindrical surface (in the case $|\nu| \geq 1$) of radius ρ_ν , both also of our choice, as we are going to explain soon. More specifically, one can have* $\exp(-2k_{I0}z)|W(\rho = \rho_\nu, \phi, z)|^2 \approx |F(z)|^2$ within a predefined longitudinal range $0 \leq z \leq L/2$, and $\exp(-2k_{I0}z)|W(\rho = \rho_\nu, \phi, z)|^2 \approx 0$ for $0 > z > L/2$.

It is important to say that while in the FW method W shapes the beam envelope, here, due to Eqs.(1,6), such modeling takes place on the pulse, i.e., $|F(z)|^2$ becomes the pulse's peak intensity pattern along the propagation, the same occurring for the transverse features, i.e., r_0 becomes the pulse's spot radius (when $\nu = 0$) and ρ_ν becomes the radius of the vortex pulse, which has a donut-shaped profile. For such modelling, the finite energy FW method [12] requires the following choices for η_m in the solution (9):

$$\eta_m = \sqrt{2} \sqrt{1 - \frac{1}{k_{R0}} \left(Q + \frac{2\pi m}{L} \right) |k(\omega_0)|}, \quad (11)$$

which implies $\zeta_m = \zeta_{r\,m} + i \zeta_{i\,m}$, with

$$\begin{cases} \zeta_{r\,m} = Q + \frac{2\pi m}{L} \\ \zeta_{i\,m} = k_{I0} \left(2 - \frac{\zeta_{r\,m}}{k_{R0}} \right), \end{cases} \quad (12)$$

where Q is a positive constant, obeying $0 \leq Q + 2\pi N/L \leq k_{R0}$ and being related to the transverse dimensions of the beam. Actually, when $\nu = 0$, the pulse spot radius, r_0 , will be approximately given by $r_0 \approx 2.4/\eta_0$ and, when $|\nu| \geq 1$, the radius of the donut-shaped vortex pulse will be approximately given by ρ_ν , which corresponds to the first positive root of $[(d/d\rho)J_\nu(\eta_0\rho)]|_{\rho=\rho_\nu} = 0$.

Yet, according to [12], the values of q and of the coefficients A_m have to be given by

$$q = \frac{2k_{R0}}{L\eta_0} \quad (13)$$

and

$$A_m = \frac{1}{L} \int_0^L \frac{F(z)}{G(z)} e^{-i\frac{2\pi}{L}mz} dz, \quad (14)$$

with

$$G(z) = e^{-k_{I0}z} \exp \left(\frac{-\eta_0^2(k_{I0} + 2q^2z)z}{2[k_{R0}^2 + (k_{I0} + 2q^2z)^2]} \right) I(z) \quad (15)$$

where $I(z)^\dagger$ is a function that is related, as we are going to see, with a possible intensity decay of $P(z, T)$.

So, by considering $W(\rho, \phi, z)$ given by Eq.(9), with Eqs.(10-15), we are ensuring that our 3D pulse solution given by Eqs.(1,6): a) can be spatially modelled on demand, presenting, as a subproduct, resistance to the diffraction and attenuation effects for long distances; b) it is endowed with OAM, being its topological charge equal to ν . The distances of diffraction and attenuation resistance, that we call

*Here, $\rho_0 \equiv 0$.

[†]The function $I(z)$ does not appear in the work of the finite energy FWs [12] because there the method deals only with beams, that is, it considers $P(z, T) = 1$.

Z_{diff} and Z_{att} , respectively, will be set by the morphological function $F(z)$ and so, as that function is set to be null for $z > L/2$, they can be considered as $Z_{diff} = Z_{att} = L/2$.

Here, we have to stress an important point. While the diffraction resistance distance can be made arbitrarily large (even experimentally it can be made hundred of times greater than the Rayleigh distance, $L_{diff} \approx \sqrt{3} k_{R0} r_0^2$), the same does not occur with the attenuation resistance distance which, according to the FW method [10], should not exceed about 10 times the penetration depth $L_{att} = 1/\alpha$ (where $\alpha = 2n_I\omega/c$ is the absorption coefficient), otherwise the lateral lobules can acquire very high intensity levels. Due to this, the parameter L , used to set up the range $0 \leq z \leq L/2$ where the morphological function $F(z)$ is non-null, is limited to values about $10/\alpha$.

Now, let us move on and make a choice to $P(z, T)$, a solution of (8) which, we expect, shall provide resistance to the dispersion effects to the resulting 3D pulse envelope. For this purpose, a natural choice is a 1D Airy-type pulse, as the finite energy Airy-exponential one given by

$$P(z, T) = \exp \left[\frac{6a(2\varepsilon\tau - Z^2) + iZ(-6a^2 - 6\varepsilon\tau + Z^2)}{12} \right] \times \text{Ai} \left(\varepsilon\tau - \frac{Z^2}{4} - iaZ \right), \quad (16)$$

where $\text{Ai}(\cdot)$ is the Airy function, $a > 0$ is a constant related with the time exponential apodization and $\varepsilon = \pm 1$ determines the direction of the Airy pulse envelope [43], which can have the smaller peaks preceding the main lobe ($\varepsilon = 1$) or the main lobe preceding the smaller peaks ($\varepsilon = -1$). In Eq.(16), we have used the normalized variables $\tau = T/T_0$ and $Z = z\beta_2/T_0^2$, with T_0 a constant equal to the initial time width of the main peak of the 1D pulse $P(z, T)$ which, depending on the value of the parameter a , can resist to the dispersion effects for distances much longer than the usual dispersion distance, $L_{disp} = T_0^2/|\beta_2|$, of ordinary gaussian pulses. A conservative estimation of the field depth, Z_{disp} , of the Airy-Exponential pulse (16) is given by

$$Z_{disp} = \sqrt{\frac{2}{a}} \frac{T_0^2}{|\beta_2|} = \sqrt{\frac{2}{a}} L_{disp}. \quad (17)$$

Although the finite energy 1D pulse solution exhibits resistance to the dispersion effects, it also exhibits a continuous intensity decay from $z = 0$. For distances smaller than Z_{disp} , it is not difficult to show that the pulse's peak intensity decays approximately according to the function

$$I(z) = \exp \left(-\frac{a\beta_2^2}{4T_0^4} z^2 \right). \quad (18)$$

The intensity decay given by (18) is taken into account (i.e., it is compensated) by $W(\rho, \phi, z)$, Eq.(9), through the coefficients A_m given by Eqs.(14,15).

In this way, with $P(z, T)$ given by Eq.(16), we are ensuring that our 3D pulse, Eqs.(1,6), is also resistant to the dispersion effects for long distances.

At this point, an important observation has to be made about the 1D pulse solution given by Eq.(16). For causality reasons, which are very well explained in [43], in the case $\varepsilon = -1$, expression (16) should not be considered for $z \geq 2T_0^3/\beta_2^2 v_g$. In our case, however, such limitation is not alarming at all because, according to our method, the morphological function $F(z)$ ensures that the resulting pulse will possess negligible intensities for $z \geq L/2$ which, in general, will be set to values much smaller than $2T_0^3/\beta_2^2 v_g$.

The final result is that the resulting 3D pulse, $\Psi(\rho, \phi, z, t)$, is given by

$$\begin{aligned}
\Psi(\rho, \phi, z, t) &= e^{-k_{I0}z} e^{ik_{R0}z} e^{-i\omega_0 t} \\
&\times \left[\frac{\exp\left(-q^2 \frac{\rho^2}{\mu}\right)}{\mu} \exp\left(-ik(\omega_0) \frac{z}{\mu}\right) \sum_{m=-N}^N A_m J_\nu\left(\eta_m \frac{\rho}{\mu}\right) e^{i\nu\phi} \exp\left(i\zeta_m \frac{z}{\mu}\right) \right] \\
&\times \left[\exp\left[\frac{6a(2\varepsilon\tau - Z^2) + iZ(-6a^2 - 6\varepsilon\tau + Z^2)}{12}\right] \text{Ai}\left(\varepsilon\tau - \frac{Z^2}{4} - iaZ\right) \right], \quad (19)
\end{aligned}$$

with μ , q , η_m , ζ_m and A_m given by Eqs.(10,13,11,12,14), being that the parameter a can be estimated from Eq.(17) once we have chosen the desired distance (Z_{disp}) of dispersion resistance for the pulse.

The new pulse solutions represented by Eq.(19), propagating in dispersive, absorbing and unguided media and carrying OAM, are resistant to the concomitant effects of diffraction, dispersion and attenuation for long distances. Actually, we can construct such pulses in such a way that we can choose where and how intense their peaks will be within the longitudinal spatial range $0 \leq z \leq L/2$.

A natural question that arises is about the generation process of these new pulses. Interestingly, this can be done in a relatively simple way, through a combination of the FW-type beams generation techniques with those for the generation of Airy-type pulses. In this sense, through a Gaussian frequency spectrum with a cubic phase [42], an Airy-Gaussian pulse is created and, thereafter, it is addressed onto a spatial light modulator, which encodes on it the FW's hologram transmission function. The desired resulting pulse can then be obtained after a 4f optical system and an iris.

3 Examples

In this section we will present two examples obtained from our theoretical method. The material medium considered here is a SF10 glass and the central (free space) wavelength used here is $\lambda_0 = 454.6\text{nm}$, which corresponds to an angular frequency $\omega_0 = 4.1464 \times 10^{15}\text{Hz}$.

At this frequency, the SF10 glass presents the following optical constants: refractive index $n = n_R + in_I$, with $n_R = 1.7554$ and $n_I = 1.5051 \times 10^{-7}$; absorption coefficient $\alpha = 0.0416\text{cm}^{-1}$, which implies an attenuation length $L_{att} = 1/\alpha = 24\text{cm}$; $\beta_1 = 6.3383 \times 10^{-9}\text{s/m}$, which implies $v_g = 1.5777 \times 10^8\text{m/s}$; dispersion coefficient $\beta_2 = 459.73\text{fs}^2/\text{mm}$.

The following two examples deal with a vortex and a non-vortex pulse, respectively, both with $\varepsilon = -1$ and a main lobe of duration $T_0 = 200\text{fs}$, which implies a dispersion length $L_{disp} = T_0^2/|\beta_2| = 8.7\text{cm}$. In the first case, the vortex pulse of topological charge $\nu = 4$ has a donut shape of radius approximately $\rho_4 = 49\mu\text{m}$, which implies a Rayleigh distance (diffraction length) $L_{diff} \approx 10\text{cm}$; in the second case, the non-vortex pulse has a spot radius $r_0 = 22.1\mu\text{m}$, which implies a Rayleigh distance $L_{diff} = \sqrt{3}k_{R0}r_0^2 \approx 2\text{cm}$. The resulting pulses will be designed to resist the effects of diffraction, dispersion and attenuation till $z = 87\text{cm}$.

3.1 First case

Let us use our solution given by Eq.(19), with $\varepsilon = -1$, to construct a diffraction-dispersion-attenuation resistant vortex pulse with topological charge $\nu = 4$, radius of the donut-shaped-pulse $\rho_4 \approx 49\mu\text{m}$, main lobe of duration $T_0 = 200\text{fs}$ and whose peak's intensity pattern along the propagation is given by a on-off-on pattern, i.e, it is dictated by $|F(z)|^2$ with:

$$F(z) = [H(z - \ell_1) - H(z - \ell_2)] + [H(z - \ell_3) - H(z - \ell_4)] , \quad (20)$$

where $H(\cdot)$ is the Heaviside function and $\ell_1 = 0$, $\ell_2 = 29\text{cm}$, $\ell_3 = 58\text{cm}$ and $\ell_4 = 87\text{cm}$. To this case, we can choose $L = 1.74\text{m}$ and, according to the desired donut-shaped-pulse's radius, the value of the parameter Q results to be $Q = 0.99999n_R\omega/c$. The morphological function $F(z)$, besides pre-defining the pulse's peak intensity behavior, also defines the diffraction-attenuation resistance distance[‡], which in this case is 87cm . To get dispersion resistance for such a distance, we have to set $a = 0.02$. Now, the resulting pulse (19) can be completely characterized through Eqs.(13-15). In this case, we use $N = 60$.

Figure 1 shows the comparison between the desired intensity pattern for the pulse's peak along the propagation, given by $|F(z)|^2$, and $|\Psi(\rho = \rho_4, \phi, z, t = t(z))|^2$, which is the evolution of the resulting pulse's peak intensity, which occurs, approximately, on $\rho = \rho_4 = 49\mu\text{m}$ and at times given by $t = -(\beta_2^2/4T_0^3)z^2 + z/v_g + 1.019T_0$ for the a given position z of the pulse's peak. We can see a good agreement between them.

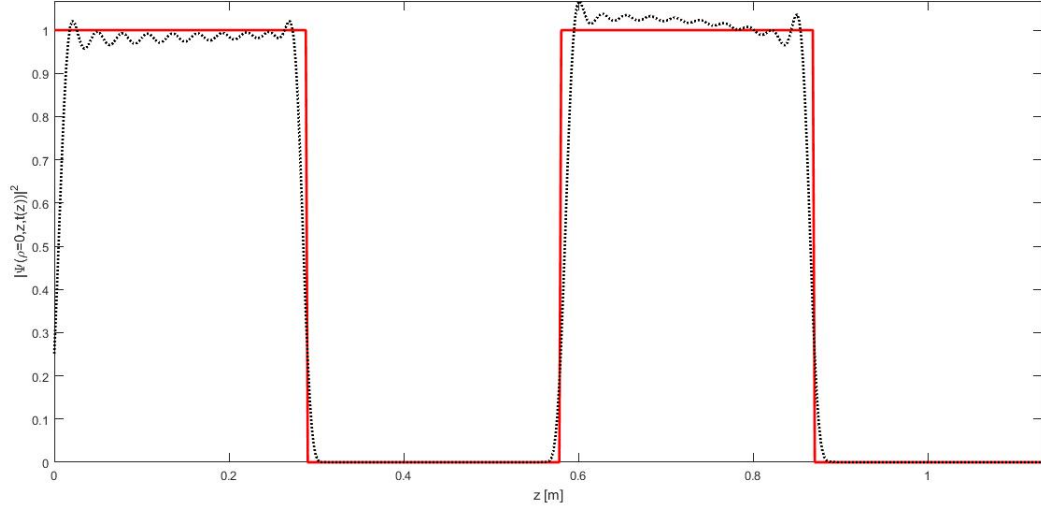


Figure 1: Comparison between the desired intensity pattern for the pulse's peak along the propagation (continuous red line), given by $|F(z)|^2$, and $|\Psi(\rho = \rho_4, \phi, z, t = t(z))|^2$, which is the evolution of the resulting pulse's peak intensity (dotted line), which occurs, approximately, on $\rho = \rho_4 = 49\mu\text{m}$ and at times $t = -(\beta_2^2/4T_0^3)z^2 + z/v_g + 1.019T_0$ for the a given position z of the pulse's peak. We can see a good agreement between them.

Figure 2 shows the temporal evolution of the resulting pulse at different distances (i.e., values of z) and considering $\rho = \rho_4 = 49\mu\text{m}$. It is evident that the pulse intensity obeys the required on-off-on behavior and also that it preserves the temporal width of its main lobe till the distance pre-defined by the morphological function $F(z)$.

Finally, Fig.3 shows the 3D pulse intensity, $|\Psi(\rho, \phi, z, t)|^2$, at nine different instants of time. The first, second and third lines of the subfigures show the pulse evolution within the ranges $\ell_1 < z < \ell_2$, $\ell_2 < z < \ell_3$ and $\ell_3 < z < \ell_4$, respectively. We can see that, in addition to the vortex pulse having the desired space-time evolution, it is resistant to the effects of the diffraction, dispersion and absorption.

[‡]According to our method, such characteristics are acquired by the resulting pulse, $\Psi(\rho, \phi, z, t) = W(\rho, \phi, z)P(z, T)$, through the function $W(\rho, \phi, z)$.

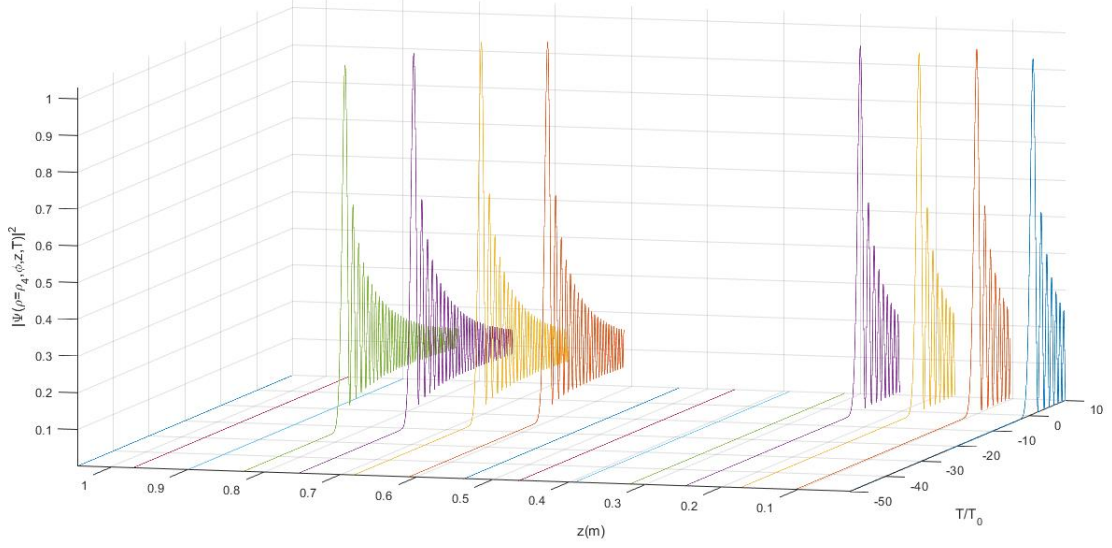


Figure 2: Temporal evolution of the resulting pulse at different distances and considering $\rho = \rho_4 = 49\mu\text{m}$. One can see that the pulse intensity obeys the required on-off-on behavior and also that it preserves the temporal width of its main lobe till a distance 10 times greater than the dispersion length of an ordinary pulse with the same temporal width.

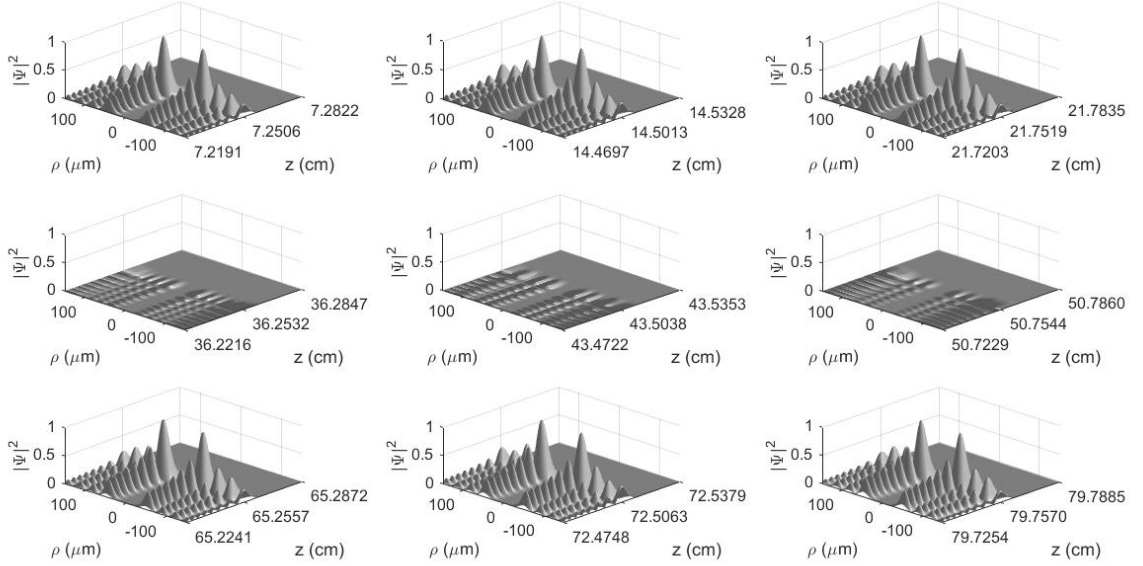


Figure 3: The 3D pulse intensity, $|\Psi(\rho, \phi, z, t)|^2$, of the first example at nine different instants of time. The first, second and third lines of the subfigures show the vortex pulse evolution within the ranges $\ell_1 < z < \ell_2$, $\ell_2 < z < \ell_3$ and $\ell_3 < z < \ell_4$, respectively. We can see that, in addition to the vortex pulse having the desired space-time evolution, it is resistant to the effects of the diffraction, dispersion and absorption.

3.2 Second case

Here, we use our solution, Eq.(19), to construct a diffraction-dispersion-attenuation resistant pulse with null topological charge, i.e. $\nu = 0$, spot radius $r_0 \approx 22\mu\text{m}$, main lobe of duration $\tau_0 = 200\text{fs}$ and whose peak's intensity pattern along the propagation is given by a ladder pattern, i.e, it is dictated by $|F(z)|^2$ with:

$$\begin{aligned} F(z) &= \sqrt{1} [H(z - \ell_1) - H(z - \ell_2)] \\ &+ \sqrt{2} [H(z - \ell_2) - H(z - \ell_3)] \\ &+ \sqrt{3} [H(z - \ell_3) - H(z - \ell_4)] , \end{aligned} \quad (21)$$

where $H(\cdot)$ is the Heaviside function and, as before, $\ell_1 = 0$, $\ell_2 = 29\text{cm}$, $\ell_3 = 58\text{cm}$ and $\ell_4 = 87\text{cm}$. To this case, we can again choose $L = 1.74\text{m}$ and, according to the desired pulse spot radius, the value of the parameter Q results to be $Q = 0.99999n_R\omega/c$. The morphological function $F(z)$, besides pre-defining the pulse's peak intensity behavior, also defines the diffraction-attenuation resistance distance, which in this case is 87cm . For obtaining dispersion resistance for such a distance, we have to set $a = 0.02$ and the resulting pulse (19) can be completely characterized through Eqs.(13-15).

Figure 4 compares the desired intensity pattern for the pulse's peak along the propagation, given by $|F(z)|^2$, with $|\Psi(\rho = 0, z, t = t(z))|^2$, the evolution of the resulting pulse's peak intensity, which occurs on $\rho = 0$ and at times $t = -(\beta_2^2/4T_0^3)z^2 + z/v_g + 1.019T_0$ for the a given position z of the pulse's peak. We can see a good agreement between them.

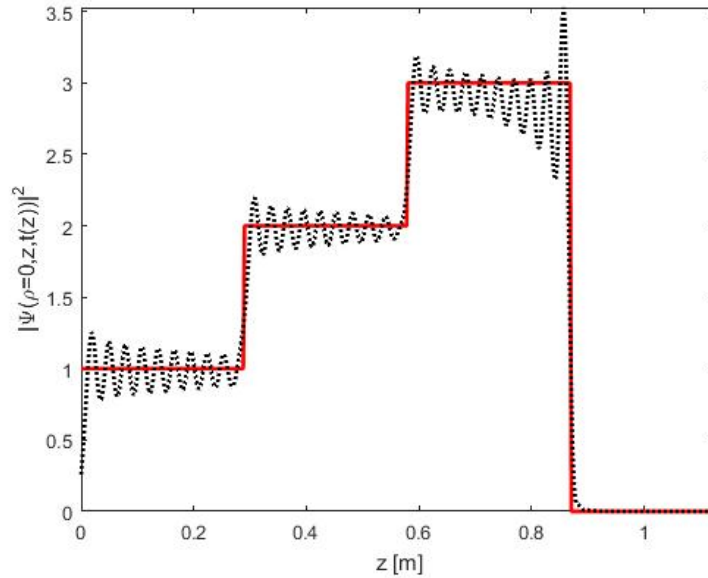


Figure 4: Comparison between the desired intensity pattern for the pulse's peak along the propagation (continuous red line), given by $|F(z)|^2$, with $|\Psi(\rho = 0, z, t = t(z))|^2$, the evolution of the resulting pulse's peak intensity (dotted line), which occurs on $\rho = 0$ and at times $t = -(\beta_2^2/4T_0^3)z^2 + z/v_g + 1.019T_0$ for the a given position z of the pulse's peak. We can see a good agreement between them

The on-axis ($\rho = 0$) temporal evolution of the resulting pulse at different distances is shown in Fig.5. It is very clear that the pulse intensity obeys the required ladder behavior, preserving the temporal width of its main lobe till the distance pre-defined by the morphological function $F(z)$.

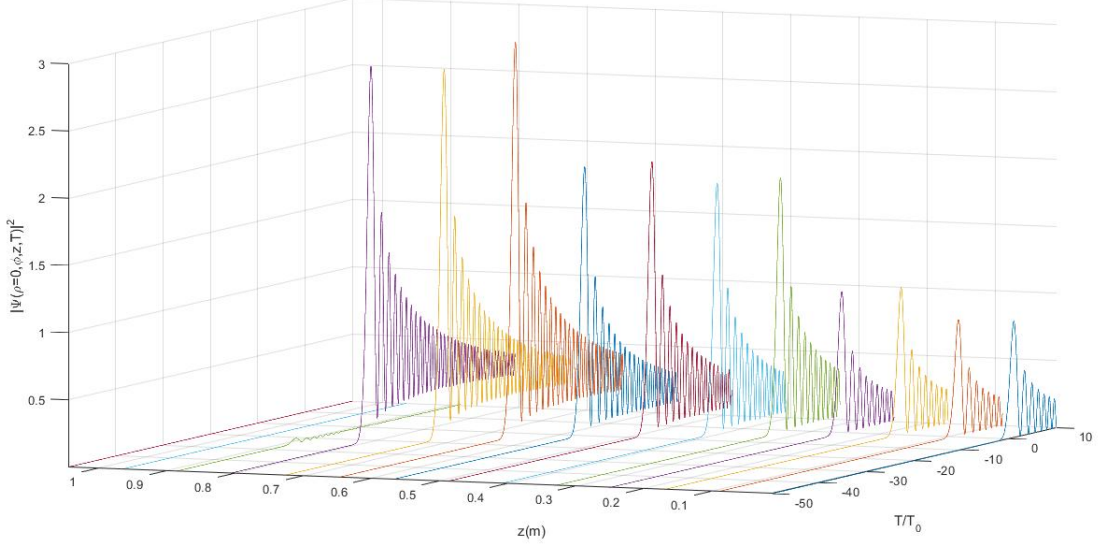


Figure 5: On-axis ($\rho = 0$) temporal evolution of the resulting pulse at different distances. One can see that the pulse intensity obeys the required ladder behavior, preserving its temporal width till a distance 10 times greater than the dispersion length of an ordinary pulse with the same temporal width.

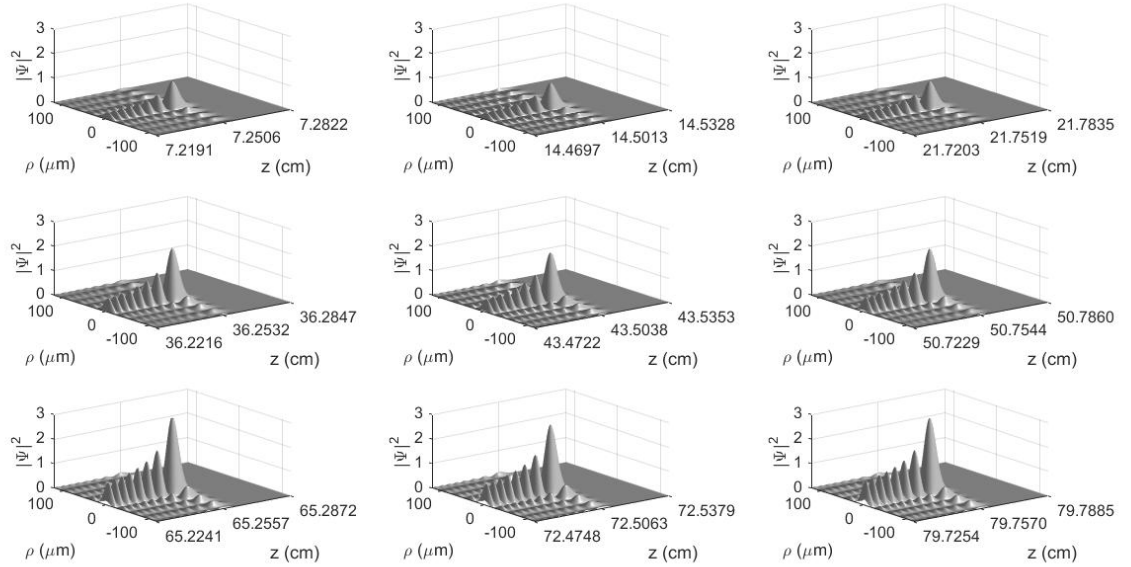


Figure 6: The 3D pulse intensity, $|\Psi(\rho, z, t)|^2$, at nine different instants of time. The first, second and third lines of the subfigures show the pulse evolution within the ranges $\ell_1 < z < \ell_2$, $\ell_2 < z < \ell_3$ and $\ell_3 < z < \ell_4$, respectively. In addition to the desired pulse's space-time evolution, one can see the pulse is resistant to the concomitant effects of diffraction, dispersion and absorption.

Finally, Fig.6 depicts the 3D pulse intensity, $|\Psi(\rho, z, t)|^2$, at nine different instants of time. The first, second and third lines of the subfigures show the pulse evolution within the ranges $\ell_1 < z < \ell_2$, $\ell_2 < z < \ell_3$ and $\ell_3 < z < \ell_4$, respectively. We can see, in addition to the desired pulse's space-time

evolution, it is resistant to the concomitant effects of diffraction, dispersion and absorption.

4 Conclusions

In this work we have developed a method capable of providing, in unguided dispersive and absorbing media, vortex pulses resistant to the three concomitant effects of diffraction, dispersion and attenuation. As a matter of fact, with our approach it is possible to perform a space-time modelling on such new pulses, i.e., it allows the choice of multiple spatial ranges where the pulse intensities can be chosen *a priori*.

Such approach is a result of a fusion between two important theoretical methodologies, one related to the so called Frozen-Wave-beams, which are non-diffracting beams whose spatial intensity pattern can be chosen *a priori* in absorbing media, the other related to the Airy-Type pulses, which are pulses resistant to the dispersion effects in material dispersive media.

The new kind of pulses can have potential applications in different fields as photonics, nonlinear optics, optical communications, optical tweezers, optical atom guiding, medicine, etc..

Acknowledgements

Thanks are due to partial support from FAPESP (under grant 2015/26444-8) and from CNPq (under grant 304718/2016-5).

References

- [1] C.J.R. Sheppard and T. Wilson, “Gaussian-beam theory of lenses with annular aperture,” *Microwaves, Optics and Acoustics*, Vol. 2, No. 4 (1978).
- [2] J.N.Brittingham, “Focus wave modes in homogeneous Maxwell’s equations: transverse electric mode,” *J. Appl. Phys.*, Vol.54, pp.1179-1189 (1983).
- [3] J.Durnin, “Exact solutions for nondiffracting beams: I. The scalar theory,” *Journal of the Optical Society of America A*, Vol.4, pp.651-654 (1987).
- [4] *Localized Waves*, edited by H.E.Hernández-Figueroa, M.Zamboni-Rached, and E.Recami (J.Wiley; Hoboken,NJ, 2008), and refs. therein.
- [5] *Non-Diffracting Waves*, edited by H.E.Hernández-Figueroa, E.Recami, and M.Zamboni-Rached (J.Wiley; Berlin, 2014), and refs. therein.
- [6] M.Zamboni-Rached, “Stationary optical wave fields with arbitrary longitudinal shape by superposing equal frequency Bessel beams: Frozen Waves,” *Opt. Express* **12**(17), 4001–4006 (2004).
- [7] M.Zamboni-Rached, E.Recami, and H.E.Hernández-Figueroa, “Theory of ‘frozen waves’: Modeling the shape of stationary wave fields,” *J. Opt. Soc. Am. A* **22**(11), 2465-2475 (2005).
- [8] T.A.Vieira, M.R.R.Gesualdi, and M.Zamboni-Rached, “Frozen waves: experimental generation,” *Opt. Lett.* **37**(11) 2034-2036 (2012).

- [9] T.A.Vieira, M.R.R.Gesualdi, M.Zamboni-Rached, and E.Recami, “Production of dynamic frozen waves: controlling shape, location (and speed) of diffraction-resistant beams”, *Opt. Lett.* **40**(24) 5834-5837 (2015).
- [10] Michel Zamboni-Rached, ”Diffraction-Attenuation resistant beams in absorbing media,” *Opt. Express* 14, 1804-1809 (2006).
- [11] A.H.Dorrah, M.Zamboni-Rached, and M.Mojahedi, “Generating attenuation-resistant frozen waves in absorbing fluid,” *Opt. Lett.* **41**(16) 3702-3705 (2015).
- [12] M.Zamboni-Rached, and M.Mojahedi, “Shaping finite-energy diffraction-and attenuation-resistant beams through Bessel-Gauss beam superposition,” *Phys. Rev. A* **92** 043839 (2015).
- [13] Michel Zamboni-Rached, Leonardo André Ambrosio, Ahmed H. Dorrah, and Mo Mojahedi, ”Structuring light under different polarization states within micrometer domains: exact analysis from the Maxwell equations,” *Opt. Express* 25, 10051-10056 (2017)
- [14] A.H.Dorrah, M.Zamboni-Rached, and M.Mojahedi, “Controlling the topological charge of twisted light beams with propagation,” *Phys. Rev. A* **93** 063864 (2016).
- [15] M.Corato Zanarella, and M.Zamboni-Rached, “Electromagnetic frozen waves with radial, azimuthal, linear, circular, and elliptical polarizations,” *Phys. Rev. A* **94** 053802 (2016).
- [16] Mateus Corato-Zanarella, Ahmed H. Dorrah, Michel Zamboni-Rached and Mo Mojahedi, “Arbitrary Control of Polarization and Intensity Profiles of Diffraction-Attenuation-Resistant Beams along the Propagation Direction,” to be published in *Phys. Rev. Applied*.
- [17] A. Sezginer, A general formulation of focus wave modes, *J. Appl. Phys.* 57, 678–683 (1985).
- [18] I.M.Besieris, A.M.Shaarawi and R.W.Ziolkowski, “A bi-directional traveling plane wave representation of exact solutions of the scalar wave equation”, *J. Math. Phys.* **30**, 1254-1269 (1989).
- [19] R. W. Ziolkowski, Localized transmission of electromagnetic energy, *Phy. Rev. A* 39, 2005–2033 (1989).
- [20] R.W. Ziolkowski, Localized wave physics and engineering, *Phys. Rev. A* 44, 3960–3984 (1991).
- [21] W. Ziolkowski, I. M. Besieris, and A. M. Shaarawi, Aperture realizations of exact solutions to homogeneous wave-equations, *J. Opt. Soc. Am. A* 10, 75 (1993), Sec. 5 and 6.
- [22] R. Donnelly and R. W. Ziolkowski, Designing localized waves, *Proc. R. Soc. London A* 440, 541–565 (1993).
- [23] J.-y.Lu and J.F.Greenleaf, “Nondiffracting X-waves: Exact solutions to free-space scalar wave equation and their finite aperture realizations”, *IEEE Trans. Ultrason. Ferroelectr. Freq. Control* **39**, 19-31, (1992).
- [24] J.-y. Lu and J. F. Greenleaf, Experimental verification of nondiffracting X-waves, *IEEE Trans. Ultrason. Ferroelectr. Freq. Control* 39, 441–446 (1992).
- [25] J.-y. Lu and J. F. Greenleaf, Ultrasonic nondiffracting transducer for medical imaging, *IEEE Trans. Ultrasonics, Ferroelectr. Freq. Control* 37(5), 438–447, (Sept. 1990).

- [26] J.-y. Lu and J. F. Greenleaf, Pulse-echo imaging using a nondiffracting beam transducer, *Ultrasound Med. Biol.* **17**(3), 265–281 (May 1991).
- [27] P. Saari and K. Reivelt, Evidence of X-shaped propagation-invariant localized lightwaves, *Phys. Rev. Lett.* **79**, 4135–4138 (1997).
- [28] E. Recami, “On localized ‘X-shaped’ Superluminal solutions to Maxwell equations”, *Physica A* **252**, 586-610 (1998), and refs. therein.
- [29] A. M. Shaarawi and I. M. Besieris, Relativistic causality and superluminal signalling using X-shaped localized waves, *J. Phys. A* **33**, 7255–7263 (2000).
- [30] Michel Zamboni-Rached, “Unidirectional decomposition method for obtaining exact localized wave solutions totally free of backward components,” *Phys. Rev. A* Vol. **79**, 013816 (2009).
- [31] H. Sönaşalg, P. Saari, “Suppression of temporal spread of ultrashort pulses in dispersive media by Bessel beam generators”, *Optics Letters* **21**, 1162-1164 (1996).
- [32] H. Sönaşalg, M. Ratsep, P. Saari, “Demonstration of the Bessel-X pulse propagating with strong lateral and longitudinal localization in a dispersive medium”, *Optics Letters* **22**, 310-312 (1997).
- [33] M. Zamboni-Rached, K. Z. Nóbrega, H. E. Hernández-Figueroa, and E. Recami, “Localized Superluminal solutions to the wave equation in (vacuum or) dispersive media, for arbitrary frequencies and with adjustable bandwidth”, *Optics Communications* **226**, 15-23 (2003).
- [34] C. Conti, and S. Trillo, “Paraxial envelope X-waves”, *Optics Letters* **28**, 1090-1093 (2003).
- [35] M. A. Porras, G. Valiulis and P. Di Trapani, “Unified description of Bessel X-waves with cone dispersion and tilted pulses”, *Physical Review E* **68**, article no.016613 (2003).
- [36] M. A. Porras, and I. Gonzalo, “Control of temporal characteristics of Bessel-X pulses in dispersive media”, *Optics Communications* **217**, 257-264 (2003).
- [37] M. A. Porras, R. Borghi, and M. Santarsiero, “Suppression of dispersion broadening of light pulses with Bessel-Gauss beams”, *Optics Communications* **206**, 235-241 (2003).
- [38] S. Longhi, “Spatial-temporal Gauss-Laguerre waves in dispersive media”, *Physical Review E* **68**, article no.066612 (2003).
- [39] G. A. Siviloglou and D. N. Christodoulides, “Accelerating finite energy Airy beams,” *Opt. Lett.* **32**(8), 979–981 (2007).
- [40] P. Saari, “Laterally accelerating airy pulses,” *Opt. Express* **16**(14), 10303–10308 (2008).
- [41] I. M. Besieris and A. M. Shaarawi, “Accelerating Airy wave packets in the presence of quadratic and cubic dispersion,” *Phys. Rev. E Stat. Nonlin. Soft Matter Phys.* **78**(4), 046605 (2008).
- [42] A. Chong, W. H. Renninger, D. N. Christodoulides, and F. W. Wise, “Airy-Bessel wave packets as versatile linear light bullets,” *Nat. Photonics* **4**(2), 103–106 (2010).
- [43] Ido Kaminer, Yaakov Lumer, Mordechai Segev, and Demetrios N. Christodoulides, “Causality effects on accelerating light pulses,” *Opt. Express* **19**, 23132-23139 (2011)

- [44] José A. Borda-Hernández, Michel Zamboni-Rached, Amr Shaarawi, and Ioannis M. Besieris, "Propagation of time-truncated Airy-type pulses in media with quadratic and cubic dispersion," *J. Opt. Soc. Am. A* 32, 1791-1796 (2015).